




ARTICLE

Cardiac MyBP-C phosphorylation regulates the Frank–Starling relationship in murine hearts

Laurin M. Hanft¹, Daniel P. Fitzsimons² , Timothy A. Hacker³, Richard L. Moss² , and Kerry S. McDonald¹ 

The Frank–Starling relationship establishes that elevated end-diastolic volume progressively increases ventricular pressure and stroke volume in healthy hearts. The relationship is modulated by a number of physiological inputs and is often depressed in human heart failure. Emerging evidence suggests that cardiac myosin-binding protein-C (cMyBP-C) contributes to the Frank–Starling relationship. We measured contractile properties at multiple levels of structural organization to determine the role of cMyBP-C and its phosphorylation in regulating (1) the sarcomere length dependence of power in cardiac myofilaments and (2) the Frank–Starling relationship in vivo. We compared transgenic mice expressing wild-type cMyBP-C on the null background, which have ~50% phosphorylated cMyBP-C (Controls), to transgenic mice lacking cMyBP-C (KO) and to mice expressing cMyBP-C that have serine-273, -282, and -302 mutated to aspartate (cMyBP-C t3SD) or alanine (cMyBP-C t3SA) on the null background to mimic either constitutive PKA phosphorylation or nonphosphorylated cMyBP-C, respectively. We observed a continuum of length dependence of power output in myocyte preparations. Sarcomere length dependence of power progressively increased with a rank ordering of cMyBP-C KO = cMyBP-C t3SA < Control < cMyBP-C t3SD. Length dependence of myofilament power translated, at least in part, to hearts, whereby Frank–Starling relationships were steepest in cMyBP-C t3SD mice. The results support the hypothesis that cMyBP-C and its phosphorylation state tune sarcomere length dependence of myofibrillar power, and these regulatory processes translate across spatial levels of myocardial organization to control beat-to-beat ventricular performance.

Introduction

Mammalian hearts exhibit a Frank–Starling relationship, wherein increased end-diastolic volume increases ventricular pressure and stroke volume. This intrinsic mechanism affords beat-to-beat regulation of cardiac contraction, which equalizes right and left heart volumes and matches ventricular supply and circulatory demand. There has been considerable research exploring the mechanisms underlying the Frank–Starling relationship, yet the molecular mechanisms remain elusive. It is evident that following a change in length of cardiac muscle, there is a significant alteration in the calcium (Ca^{2+}) sensitivity of force (Allen and Kurihara, 1982), i.e., changes in the responsiveness of the myofilaments to Ca^{2+} (reviewed in Fuchs and Martyn, 2005). Length-dependent changes in the activation of cardiac myofilaments appear to occur within a few milliseconds of the length change (Mateja and de Tombe, 2012), which implies that the length change induces a strain-dependent rearrangement of the thick and thin filament lattice and/or individual contractile and regulatory proteins. One hypothesis

proposed previously is that increased sarcomere length (SL) reduces the lateral separation of the thick and thin filaments, thereby increasing the effective concentration of cross-bridges in the vicinity of thin filaments. Consistent with this idea, compression of the lattice at short SL has been shown to increase Ca^{2+} sensitivity of force to values similar to those observed at long SLs (McDonald and Moss, 1995; Wang and Fuchs, 1995). However, this hypothesis has been challenged by the finding that small changes in SL that elicited negligible changes in interfilament lattice spacing caused changes in force (Konhilas et al., 2002). This result suggests an alternative or complementary possibility that changes in myofilament strain exclusively produce a mechanical signal to increase force generation. Studies using x-ray diffraction and electron density mapping reported length-dependent changes in meridional reflections produced by myosin, thin filament proteins, and an as yet unidentified molecule than spans the lateral separation of thick and thin filaments (Ait-Mou et al., 2016). These length-dependent

¹Department of Medical Pharmacology and Physiology, University of Missouri, Columbia, MO; ²Department of Cell and Regenerative Biology, University of Wisconsin-Madison, Madison, WI; ³Department of Medicine, University of Wisconsin-Madison, Madison, WI.

Correspondence to Kerry S. McDonald: mcdonaldks@missouri.edu

This work is part of a special collection on myofilament function and disease.

© 2021 Hanft et al. This article is distributed under the terms of an Attribution–Noncommercial–Share Alike–No Mirror Sites license for the first six months after the publication date (see <http://www.rupress.org/terms/>). After six months it is available under a Creative Commons License (Attribution–Noncommercial–Share Alike 4.0 International license, as described at <https://creativecommons.org/licenses/by-nc-sa/4.0/>).

structural changes varied with the titin isoform, which implicates titin as an important component of the length-sensing mechanism (Ait-Mou et al., 2016). However, the question remains as to how titin molecules communicate with proteins of the thin and thick filaments for such rapid and integrated contractile response.

One plausible sensor of sarcomere strain is the 140–150-kD cardiac isoform of myosin-binding protein-C (cMyBP-C), which is localized to the proximal two thirds of each half thick filament and has sufficient length to span the distance between the thick and thin filaments (Lee et al., 2015). Furthermore, there is evidence that cMyBP-C binds to myosin and actin in a phosphorylation-dependent manner (Mun et al., 2011; Belknap et al., 2014; Mun et al., 2014; Harris et al., 2016; Mun et al., 2016; Ponnamp et al., 2019). Taken together, these findings implicate a significant role for cMyBP-C and its phosphorylation state as a molecular regulator of SL-dependent contractile properties. Our study employed complementary approaches to test the hypothesis that cMyBP-C serves as an interfilament length sensor that integrates mechano-transduction systems to tune myofibrillar force and power, which translates to ventricular function curves (i.e., Frank-Starling relationships).

Materials and methods

Experimental animals

Male and female transgenic mice (5–13 mo old; background strain: 129S1/SvIm) were used for mechanical and physiological measurements. Genetically engineered mouse lines were established in the Laboratory of Animal Resource in the University of Wisconsin School of Medicine and Public Health at the University of Wisconsin-Madison. The four groups were cMyBP-C wild-type (Control; 6–12 mo old), phospho-mimetic (cMyBP-C t3SD; 5–13 mo old), phospho-null (cMyBP-C t3SA; 7–11 mo old), and cMyBP-C knockout (KO; 6–13 mo old). There were no statistically significant age differences between groups. The transgenic mice lines have been well characterized as models for cMyBP-C KO or the constitutively nonphosphorylated and phosphorylated states of cMyBP-C (Harris et al., 2002; Korte et al., 2003; Stelzer et al., 2006, 2007; Luther et al., 2008; Tong et al., 2008, 2015; Chen et al., 2012; Colson et al., 2012; Rosas et al., 2015). Since the cMyBP-C wild-type (cMyBP-C Control), phospho-mimetic (cMyBP-C t3SD), or phospho-null (cMyBP-C t3SA) proteins are expressed on a null background, these transgenic mice provide a unique model system in which cardiac myofilaments contain only the genetically engineered cMyBP-C molecules. The modified proteins have been shown to properly incorporate into the myofibril with expression levels of 75–85% relative to cMyBP-C levels in a 129S1/SvIm mouse (Tong et al., 2008; Rosas et al., 2015). In addition, the phosphorylation status of cMyBP-C in the Control group is ~50%, and the phosphorylation status of other sarcomeric proteins was similar across mouse lines (Korte et al., 2003; Tong et al., 2008; Rosas et al., 2015). All procedures involving animals were performed in accordance with the Animal Care and Use Committee of the University of Wisconsin and the University of Missouri.

Solutions

Relaxing solution for permeabilized cardiac myocytes contained 1 mM dithiothreitol, 100 mM KCl, 10 mM imidazole, 2.0 mM EGTA, 4.0 mM ATP, and 1 mM (free, 5 total) MgCl_2 . Minimal Ca^{2+} activating solution (pCa ($-\log[\text{Ca}^{2+}]$) 9.0) for experimental protocol contained 7.00 mM EGTA, 20 mM imidazole, 5.42 mM MgCl_2 , 72.37 mM KCl, 0.016 mM CaCl_2 , 14.5 mM phosphocreatine (PCr), and 4.7 mM ATP. Maximal Ca^{2+} activating solution (pCa 4.5) for experimental protocol contained 7.00 mM EGTA, 20 mM imidazole, 5.26 mM MgCl_2 , 60.25 mM KCl, 7.01 mM CaCl_2 , 14.5 mM PCr, and 4.81 mM ATP. A range of Ca^{2+} concentrations for experiments were prepared by varying combinations of maximal and minimal Ca^{2+} solutions. Preactivating solution contained 0.5 mM EGTA, 20 mM imidazole, 5.42 mM MgCl_2 , 98.18 mM KCl, 0.016 mM CaCl_2 , 14.5 mM PCr, and 4.8 mM ATP.

Permeabilized cardiac myocyte preparations

A total of 29 permeabilized cardiac myocyte preparations were used from five Control and seven (t3SD), five (t3SA), and six cMyBP-C KO hearts (i.e., one or two myocyte preparations per heart). Permeabilized cardiac myocytes were obtained by mechanical disruption of mouse hearts as described previously (McDonald, 2000a). Mice were anesthetized by inhalation of isoflurane (20% vol/vol in olive oil), and hearts were excised and rapidly placed in ice-cold relaxing solution. The left ventricle was separated from the right ventricle and dissected from the atria, cut into 2–3-mm pieces, and further disrupted for 5 s in a Waring blender. The resulting suspension of cells was centrifuged for 105 s at 165 $\times g$, after which the supernatant fluid was discarded. The myocytes were permeabilized by suspending the cell pellet for 2 min in 0.3% ultrapure Triton X-100 (Pierce Chemical Co.) in cold relaxing solution. The permeabilized myocytes were washed twice with cold relaxing solution, suspended in 10 ml of relaxing solution, and kept on ice for the experimental day.

Experimental apparatus

The experimental apparatus for mechanical measurements of permeabilized myocyte preparations was described previously (McDonald, 2000a). A permeabilized cardiac myocyte preparation was mounted between a force transducer, and motor and contractile properties were measured. Cardiac myocyte preparations were attached by placing the ends of a myocyte into stainless steel troughs (25 gauge), and ends were secured by overlaying a 0.5-mm length of 4–0 monofilament nylon suture (Ethicon, Inc.) and tightening the suture into the troughs with loops of 10–0 monofilament (Ethicon, Inc.; Fig. 1 A). The attachment procedure was performed under a stereomicroscope (90 \times zoom) using finely shaped forceps (McDonald, 2000a).

Prior to mechanical measurements, the experimental apparatus was mounted on the stage of an inverted microscope (model IX-70; Olympus Instrument Co.). Force measurements were made using a capacitance-gauge transducer (Model 403-sensitivity of 20 mV/mg [plus a 10 \times amplifier] and resonant frequency of 600 Hz; Aurora Scientific, Inc.). Length changes were introduced using a DC torque motor (model 308; Aurora Scientific, Inc.) driven by voltage commands from a personal computer via a 16-bit digital-to-analogue converter (AT-MIO-16E-1;

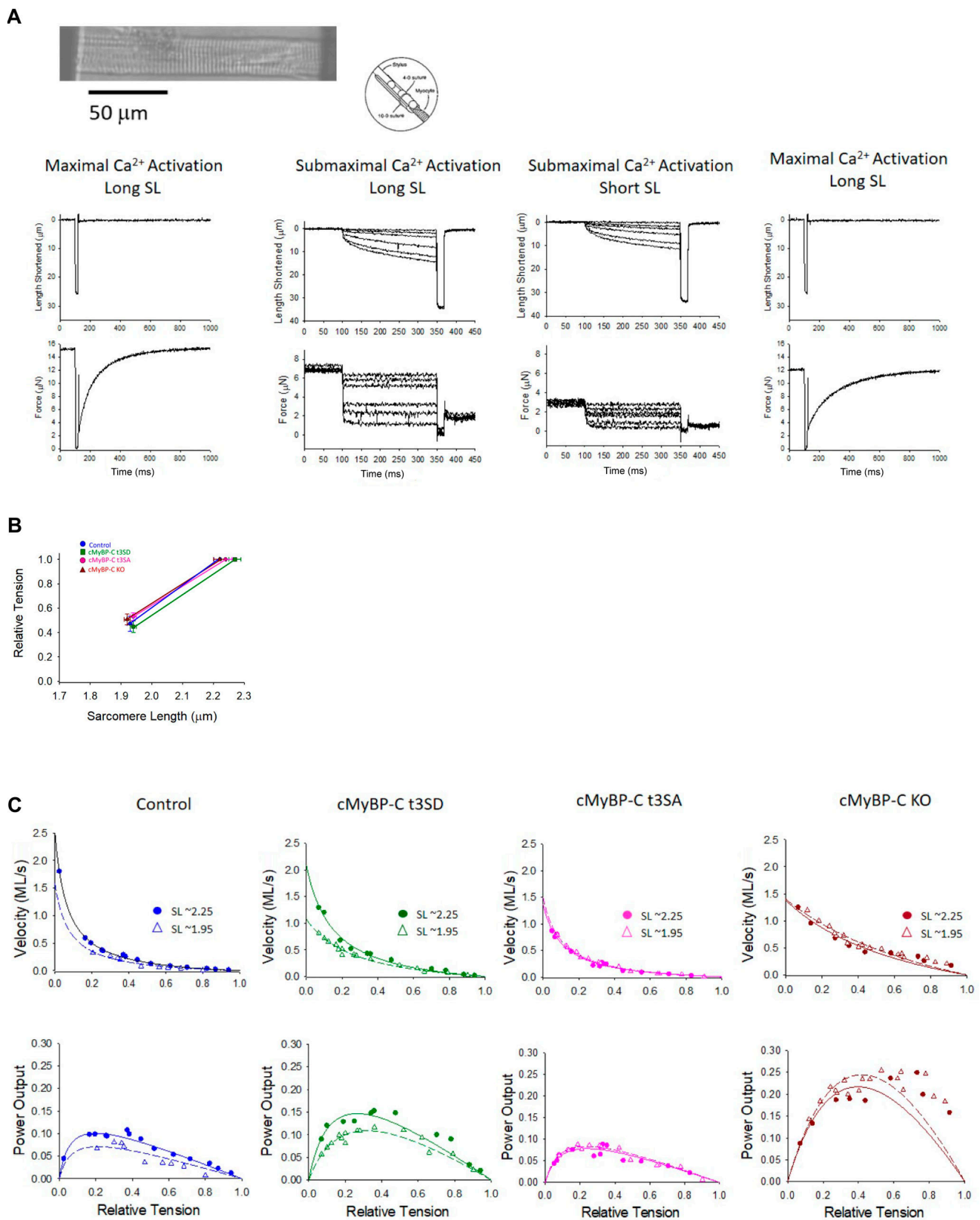


Figure 1. SL dependence of tension, loaded shortening, and power output in permeabilized cardiac myocytes from Control, phospho-mimetic cMyBP-C t3SD, phospho-null cMyBP-C t3SA, and cMyBP-C KO mice. (A) Top: A photomicrograph of representative mouse permeabilized cardiac myocyte preparation and a schematic showing the permeabilized myocyte attachment. **Bottom:** Length and force traces during maximal Ca^{2+} activation at the beginning of the experiment, followed by representative length traces during a series of force clamps at both long and short SLs during half-maximal Ca^{2+}

activation, and a final length and force trace during maximal Ca^{2+} activation. **(B)** Summary data of normalized SL–tension relationships during approximately half-maximal Ca^{2+} activation from the four groups. Data points are mean \pm SEM. **(C)** Representative normalized force-velocity and power-load curves at approximately half-maximal Ca^{2+} activations at long and short SLs from one myocyte preparation from each group.

National Instruments Corp.). Force and length signals were digitized at 1 kHz and stored on a personal computer using LabView for Windows (National Instruments Corp.). SL was set using an IonOptix SarcLen system, which was done with a fast-Fourier transform algorithm of the video image of the myocyte.

Force-velocity and power-load measurements

The protocol to obtain force-velocity and power-load measurements has been described in detail (McDonald, 2000b), and all measurements were done at $15^{\circ}\text{C} \pm 1^{\circ}\text{C}$. To determine SL dependence of loaded shortening and power output, the following protocol was used. An attached myocyte was adjusted to an SL of $\sim 2.25\ \mu\text{m}$ and then transferred into maximal Ca^{2+} activating solution (pCa 4.5) and allowed to develop maximal steady-state isometric force. The myocyte was transferred to a submaximal Ca^{2+} activating solution that yielded approximately half-maximal Ca^{2+} activated force at long SL, and then a series of subisometric force clamps were applied to determine isotonic shortening velocities. The isotonic force was maintained using a servo system for 150–250 ms, and muscle length changes during this time were monitored (Fig. 1 A shows examples of force clamps and corresponding muscle length traces). Following the force clamp, the myocyte was slackened to near zero force to estimate the relative load sustained during the isotonic shortening, after which the myocyte was reextended to its starting length. The myocytes were kept in submaximal Ca^{2+} activating solution 3–5 min, during which 10–20 force clamps were performed. Following force-velocity measurements at long SL, the SL was then shortened to $\sim 1.95\ \mu\text{m}$, and a second force-velocity relationship was obtained using the same submaximal Ca^{2+} activating solution. The SL range is thought to span the working SL range in vivo (Pollack and Huntsman, 1974; Grimm et al., 1980; Guccione et al., 1997; Chung et al., 2018). A final force measurement was made at long SL in pCa 4.5 solution, and if it was found to be below 70% of initial maximum tension, data from that myocyte were discarded.

In vivo measurements of ventricular function curves (i.e., Frank–Starling relationships)

Mice were anesthetized with 1% isoflurane and 99% oxygen and placed on a heated platform. In vivo Frank–Starling relationships (i.e., stroke volume versus end-diastolic volume relations) were obtained by performing sequential M-mode echocardiography (Vevo 770; Visual Sonics) of the left ventricle of anesthetized mice in conjunction with a 50- μl stepwise blood volume withdrawal/expansion protocol. M-mode measurements were used to obtain end-diastolic and end-systolic volumes along with wall thickness and were then used to calculate stroke volumes. For this protocol, a baseline M-mode echocardiogram was obtained, and then blood was first withdrawn from the jugular vein in 50- μl increments, and an M-mode recording was made within 1 min of each 50- μl withdrawal. This sequence continued until 200 μl of blood was extracted. Once a total of 200 μl of blood

was extracted, 300 μl saline was added to the extracted blood. As soon as possible after mixing (within 2–3 min of the last withdrawal), this 500 μl of total blood was then injected back into the jugular vein in 50- μl increments with an M-mode recording occurring after each 50- μl injection, with the same timing as the withdrawals. A single operator performed and read all echo measurements on a Visual Sonics Vevo 770 using a 25-MHz probe.

Data and statistical analysis

Myocyte length traces, force-velocity curves, and power-load curves were analyzed as previously described (McDonald, 2000a). Myocyte length and SL traces during loaded shortening were fit to a single decaying exponential equation:

$$L = Ae^{-kt} + C,$$

where L is cell length at time t , A and C are constants with dimensions of length, and k is the rate constant of shortening ($k_{\text{shortening}}$). Velocity of shortening at any given time, t , was determined as the slope of the tangent to the fitted curve at that time point. In this study, loaded shortening velocities were calculated at the onset of the force clamp ($t = 0$ ms) and were normalized to long SL ($\sim 2.25\ \mu\text{m}$).

Hyperbolic force-velocity curves were fit to the relative force-velocity data using the Hill equation (Hill, 1938)

$$(P + a)(V + b) = (P_0 + a)b,$$

where P is force during shortening at velocity V ; P_0 is the maximal isometric force; and a and b are constants with dimensions of force and velocity, respectively. Force-velocity data were normalized to isometric force to illustrate condition effects on loaded shortening velocity. Power-load curves were obtained by multiplying force \times velocity at each relative load on the force-velocity curve, and statistical analysis compared peak normalized power output (PNPO) values, which were obtained by multiplying relative force at optimum power \times velocity at optimum power. Curve fitting was performed using a customized program written in Qbasic, as well as commercial software (SigmaPlot).

The experimental data between groups were compared by one-way ANOVA and post hoc analysis using a Student–Newman–Keuls test. In vivo sex differences were tested by two-way ANOVA. $P < 0.05$ was accepted as a statistically significant difference. N is the number of mice for myocyte mechanics (Fig. 1 and Table 1) and in vivo mice (Fig. 2 and Table 3). n is the number of permeabilized cardiac myocyte preparations (Fig. 1 and Table 1). Values are expressed as means \pm SEM.

Results

SL dependence of tension, loaded shortening, and power output of transgenic mouse permeabilized cardiac myocyte preparations

To ascertain the role of cMyBP-C and its phosphorylation state on length-dependent contraction, four groups of cMyBP-C

Table 1. Transgenic mouse permeabilized cardiac myocyte preparations at long SL

| Cardiac myocyte preparations | Length (μm) | Width (μm) | SL (μm) | Passive tension ($\text{kN}\cdot\text{m}^{-2}$) | Maximum force (μN) | Maximum tension ($\text{kN}\cdot\text{m}^{-2}$) | pCa for half-max. tension | Relative tension half-max. pCa |
|----------------------------------|--------------------------|-------------------------|----------------------|---|---------------------------------|---|---------------------------|--------------------------------|
| Control ($n = 5$) $n = 6$ | 128 \pm 14 | 22 \pm 2 | 2.22 \pm 0.02 | 2.29 \pm 0.27 | 16.5 \pm 1.9 | 66 \pm 13 | 5.92 \pm 0.04 | 0.47 \pm 0.03 |
| cMyBP-C 3tSD ($n = 7$) $n = 8$ | 140 \pm 10 | 22 \pm 2 | 2.27 \pm 0.02 | 1.79 \pm 0.21 | 16.3 \pm 2.0 | 63 \pm 6 | 5.95 \pm 0.03 | 0.47 \pm 0.02 |
| cMyBP-C 3tSA ($n = 5$) $n = 7$ | 122 \pm 9 | 21 \pm 1 | 2.24 \pm 0.02 | 1.97 \pm 0.36 | 12.7 \pm 0.9 | 53 \pm 7 | 5.94 \pm 0.05 | 0.52 \pm 0.02 |
| cMyBP-C KO ($n = 6$) $n = 7$ | 150 \pm 17 | 25 \pm 2 | 2.22 \pm 0.02 | 1.66 \pm 0.16 | 16.8 \pm 1.8 | 51 \pm 7 | 5.91 \pm 0.03 | 0.48 \pm 0.03 |

Values are means \pm SEM.

constitutive transgenic mice were used. The four groups were cMyBP-C wild-type (Control), phospho-mimetic (cMyBP-C t3SD), phospho-null (cMyBP-C t3SA), and cMyBP-C KO, from which permeabilized single cardiac myocyte preparations were isolated. Table 1 and Table 2 show permeabilized cardiac myocyte preparation characteristics and contractile properties, respectively, from the four transgenic mouse groups. Cardiac myocyte preparations exhibited similar sizes, passive tension, and maximal Ca^{2+} activated tension among all groups. In addition, SL dependence of relative tension was similar between groups (Fig. 1 B) over an SL of $\sim 2.25 \mu\text{m}$ to $\sim 1.95 \mu\text{m}$. Next, the SL dependence of force-velocity and power-load curves was assessed. Fig. 1 C shows representative normalized force-velocity and power-load curves at half-maximal Ca^{2+} activation at long ($\sim 2.25 \mu\text{m}$) and short ($\sim 1.95 \mu\text{m}$) SLs in

permeabilized cardiac myocytes from Control, phospho-mimetic cMyBP-C t3SD, phospho-ablated cMyBP-C t3SA, and cMyBP-C KO mice. SL dependence of power was quantified by the difference between peak power at long SL versus short SL (ΔPNPO ; Fig. 2). There was a continuum of length dependence of power output between the different myocyte preparation groups; SL dependence of power progressively increased with a rank ordering of cMyBP-C KO = cMyBP-C t3SA < Control < cMyBP-C t3SD. A prominent finding was a marked increase of SL dependence of PNPO in cMyBP-C t3SD myocyte preparations ($P < 0.001$ compared with the other three groups). These results indicate that cMyBP-C residue-specific modifications play a prominent role in regulating length-dependent myofilament work capacity.

In vivo Frank-Starling relationships

The next series of experiments tested whether SL dependence of myofilament power translated to in vivo hearts. For these experiments, ventricular function relationships (i.e., Frank-Starling relationships) were characterized by a volume expansion protocol in tandem with echocardiography in transgenic mice from the four groups. Baseline M-mode echocardiographic measurements are shown in Table 3, and representative M-mode echocardiograms are shown in Fig. 3 A. In accordance with classic descriptions of the Frank-Starling relationships, step-wise volume expansion via saline injection and its consequent increase in end-diastolic volume generally elevated stroke volume in all four groups (Fig. 3 B). Notably, cMyBP-C t3SD mice were considerably more sensitive to end-diastolic volumes, exhibiting significantly steeper Frank-Starling relationships (Fig. 3 B). The mean slope of the Frank-Starling relationship was significantly greater in the cMyBP-C t3SD mice than in the three other groups (Fig. 4), consistent with results observed at the myofilament level. Mean slope values were Control, 0.304 ± 0.046 ; cMyBP-C t3SD, 0.496 ± 0.052 ; cMyBP-C t3SA, 0.224 ± 0.049 ; and cMyBP-C KO, 0.260 ± 0.078 (Fig. 4). There was no difference in Frank-Starling relationships between female and male mice. Together, these results suggest that regulation of myofilament mechanics by cMyBP-C and its phosphorylation state translate, at least in part, across levels of spatial organization from single myocytes to intact

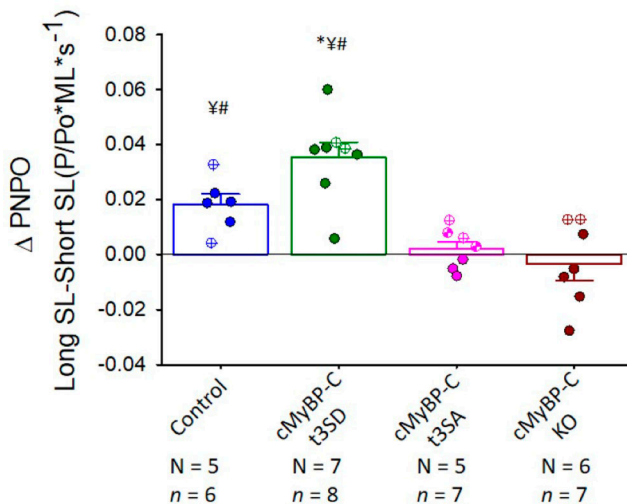


Figure 2. SL dependence of power progressively increased from cMyBP-C KO = cMyBP-C t3SA < Control < cMyBP-C t3SD. Summary data for the change in PNPO from long SL to short SL (ΔPNPO) for individual cardiac myocyte preparations from the four groups. Bars indicate mean \pm SEM. N = number of mouse hearts. n = number of permeabilized cardiac myocyte preparations. Open circles with the same middle symbol indicate permeabilized cardiac myocyte preparations from the same heart. *, $P < 0.05$ versus Control. $\#$, $P < 0.05$ versus cMyBP-C t3SA. $\#$, $P < 0.05$ versus cMyBP-C KO. ML, muscle length; P/P_o , force relative to isometric force.

Table 2. Permeabilized cardiac myocyte preparation force-velocity and power-load characteristics at long and short SL during submaximal Ca^{2+} activation

| | SL (μm) | a/P_o | F_{opt} (P/P _o) | V_{opt} (ML·s ⁻¹) | V_{max} (ML·s ⁻¹) | Peak absolute power output ($\mu\text{W mg}^{-1}$) | PNPO (P/P _o ML·s ⁻¹) |
|---------------------|----------------------|--------------------------|-------------------------------|---------------------------------|---------------------------------|--|---|
| Control | | | | | | | |
| Long SL | 2.22 ± 0.02 | 0.16 ± 0.04 | 0.26 ± 0.03 | 0.44 ± 0.04 | 1.84 ± 0.16 | 3.52 ± 0.98 | 0.118 ± 0.017 |
| Short SL | 1.93 ± 0.01 | 0.23 ± 0.05 | 0.29 ± 0.02 | 0.35 ± 0.05 | 1.23 ± 0.18 | 1.36 ± 0.35 | 0.100 ± 0.017 |
| cMyBP-C 3tSD | | | | | | | |
| Long SL | 2.27 ± 0.02 | 0.21 ± 0.04 | 0.28 ± 0.02 | 0.48 ± 0.04 | 1.71 ± 0.14 | 3.61 ± 0.58 | 0.135 ± 0.018 |
| Short SL | 1.94 ± 0.01 | 0.23 ± 0.04 | 0.29 ± 0.02 | 0.33 ± 0.04 | 1.14 ± 0.10 | 1.27 ± 0.27 | 0.099 ± 0.015 |
| cMyBP-C 3tSA | | | | | | | |
| Long SL | 2.24 ± 0.02 | 0.27 ± 0.05 | 0.31 ± 0.02 | 0.38 ± 0.06 | 1.30 ± 0.19 | 2.94 ± 0.73 | 0.118 ± 0.019 |
| Short SL | 1.94 ± 0.01 | 0.28 ± 0.05 | 0.31 ± 0.02 | 0.37 ± 0.05 | 1.23 ± 0.14 | 1.48 ± 0.31 | 0.116 ± 0.020 |
| cMyBP-C KO | | | | | | | |
| Long SL | 2.22 ± 0.02 | 0.66 ± 0.21 ^a | 0.36 ± 0.03 | 0.43 ± 0.04 | 1.28 ± 0.17 | 3.10 ± 0.39 | 0.154 ± 0.021 |
| Short SL | 1.92 ± 0.01 | 0.96 ± 0.35 ^a | 0.37 ± 0.03 | 0.41 ± 0.05 | 1.16 ± 0.10 | 1.56 ± 0.29 | 0.157 ± 0.026 |

Values are mean ± SEM. a, constant with dimension of force from the second equation relative to isometric force (P_o); F_{opt} , relative force at peak power; ML, muscle length; P/P_o, force relative to isometric force; V_{opt} , velocity at F_{opt} .

^aP < 0.05 versus Control, cMyBP-C 3tSD, and cMyBP-C 3tSA.

beating hearts and provide a mechanistic basis for how end-diastolic volume controls ventricular stroke output (i.e., the Frank-Starling relationship).

Discussion

The Frank-Starling relationship was described over a century ago as an intrinsic mechanism for beat-to-beat regulation, whereby increased end-diastolic volume increases stroke volume, and continues as an area of intensive study due to its critical importance in heart function. For example, reduced functional reserve due to a depressed Frank-Starling relationship underlies human heart failure (Braunwald and Ross, 1964; Jacob et al., 1992; Schwinger et al., 1994; Holubarsch et al., 1996). Mechanistically, cardiac myofibrils exhibit length-dependent activation (Fuchs and Martyn, 2005), comprising the Frank-

Starling Relationship; however, the molecular mechanisms that evoke altered contraction in response to length changes remain elusive. The mechanism(s) that determine the Frank-Starling relationship likely involve physical factors at the level of the sarcomere, including alterations in interfilament lattice spacing (Fuchs and Martyn, 2005) and myosin cross-bridge orientation (Ait-Mou et al., 2016), perhaps mediated by titin (Cazorla et al., 2001; Fukuda et al., 2003). Length-dependent changes in the activation of cardiac myofilaments occur within a few milliseconds (Mateja and de Tombe, 2012), which implies a nearly instantaneous rearrangement of the myofilament lattice. Evidence suggests that thin filament proteins are involved in length-dependent activation. For example, the affinity of cardiac troponin C for Ca^{2+} increases with length due to a greater number of force-generating cross-bridges (Hofmann and Fuchs, 1987b, 1987a). Also, striated muscle troponin I (TnI) isoforms

Table 3. Echocardiography parameters of transgenic mice

| | Number of animals (n) | Body weight (g) | LVID; diastole (mm) | LVID; systole (mm) | LVPW; diastole (mm) | LVPW; systole (mm) | LVAW; diastole (mm) | LVAW; systole (mm) |
|--------------|-----------------------|-----------------|---------------------|--------------------------|---------------------|--------------------|---------------------|--------------------|
| Control | n = 14 | 33 ± 2 | 4.91 ± 0.19 | 3.94 ± 0.21 | 0.67 ± 0.02 | 0.91 ± 0.04 | 0.67 ± 0.02 | 0.90 ± 0.04 |
| cMyBP-C 3tSD | n = 12 | 29 ± 2 | 4.45 ± 0.23 | 3.42 ± 0.27 ^a | 0.67 ± 0.01 | 0.89 ± 0.05 | 0.68 ± 0.01 | 0.88 ± 0.03 |
| cMyBP-C 3tSA | n = 11 | 30 ± 2 | 5.05 ± 0.10 | 4.41 ± 0.11 | 0.66 ± 0.01 | 0.77 ± 0.01 | 0.65 ± 0.01 | 0.76 ± 0.01 |
| cMyBP-C KO | n = 11 | 26 ± 1 | 4.83 ± 0.21 | 4.17 ± 0.21 | 0.70 ± 0.04 | 0.86 ± 0.06 | 0.69 ± 0.03 | 0.80 ± 0.03 |

Values are means ± SEM.

LVAW, left ventricular anterior wall; LVID, left ventricular inner diameter; LVPW, left ventricular posterior wall.

^aP < 0.05 versus cMyBP-C 3tSA.

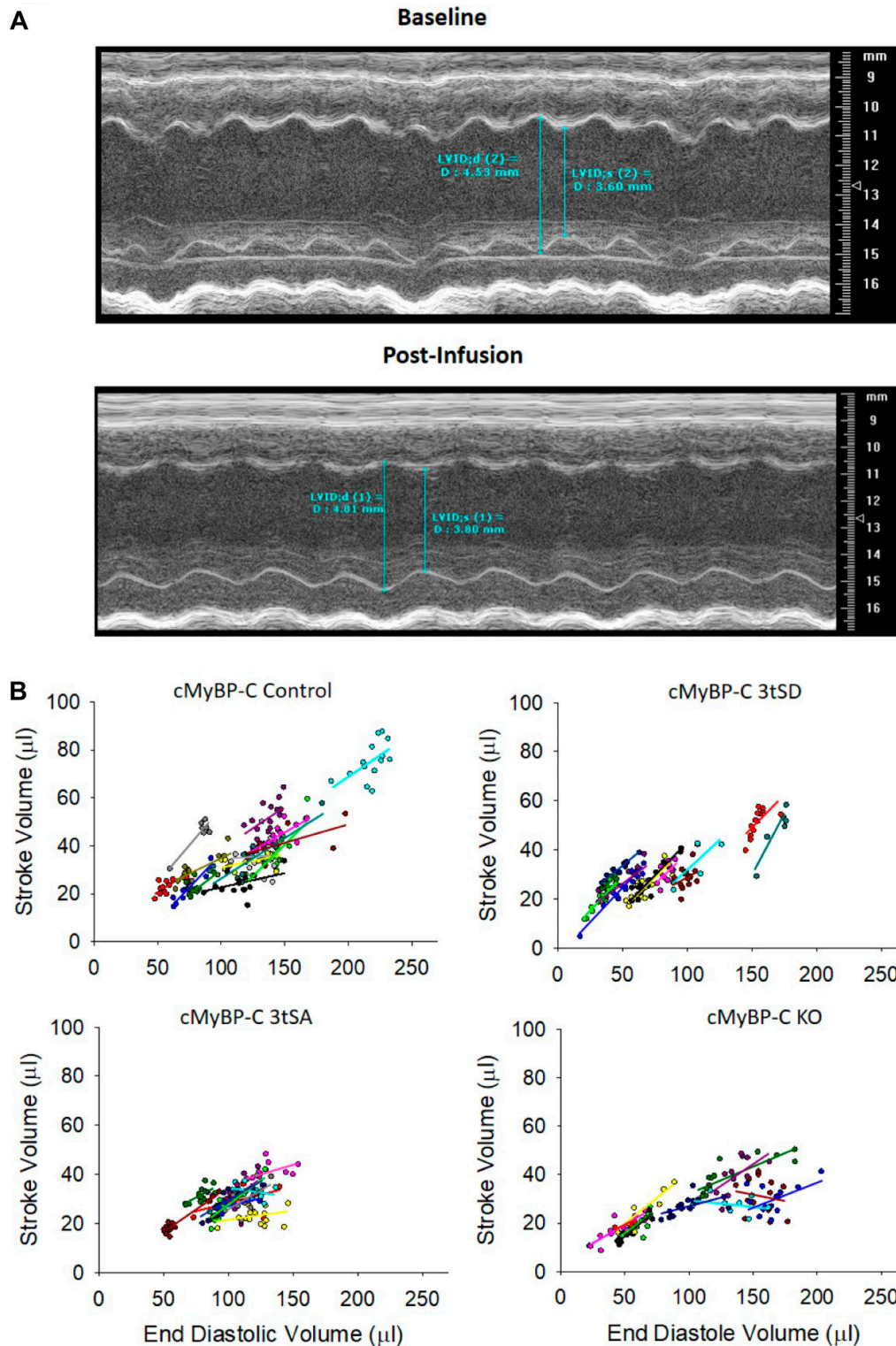


Figure 3. **In vivo assessment of Frank-Starling relationships using simultaneous volume expansion and echocardiography.** (A) Representative M-mode echocardiograms before and after end-diastolic volume change. Arrows indicate measures of left ventricular inner diameter at end-diastole and end-systole (LVID;d and LVID;s). (B) Stepwise volume expansion via saline injection into the jugular vein during continuous echocardiographic imaging in anesthetized mice revealed cMyBP-C t3SD mice have steeper Frank-Starling relationships than the other three groups. The individual relationships are plotted for each mouse, and data points obtained from each mouse are shown in a separate color.

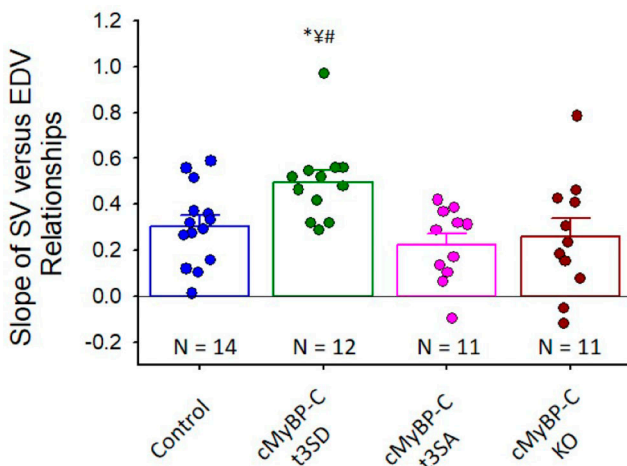


Figure 4. **The mean slope of the Frank-Starling relationship was significantly greater in the cMyBP-C t3SD mice than in the three other groups.** Summary data of the stroke volume (SV) versus end-diastolic volume (EDV) slopes are shown for each of the four groups. Bars indicate means \pm SEM. *, $P < 0.05$ versus Control. †, $P < 0.05$ versus cMyBP-C t3SA. #, $P < 0.05$ versus cMyBP-C KO.

correlate with length dependence of Ca^{2+} sensitivity of force (Konhilas et al., 2003). Furthermore, a threonine residue at position 144 of cardiac TnI (cTnI) modulates length dependence of Ca^{2+} sensitivity of force, suggesting a role for the cTnI inhibitory domain in length-dependent activation (Tachampa et al., 2007; de Tombe et al., 2010). In addition, PKA phosphorylation of cTnI increases length-dependent activation (Konhilas et al., 2003; Hanft and McDonald, 2010). Hanft et al. (2013) went on to show that PKA phosphorylation of cTnI N-terminal serines or site-directed mutagenesis of serines 22/23 to aspartic acid was sufficient to steepen length-tension relationships of rat slow-twitch skeletal muscle fibers.

Thick filament proteins also appear to regulate length dependence of force. Consistent with this idea, PKA phosphorylation of cMyBP-C per se enhances length dependence of both Ca^{2+} sensitivity of force and rates of force in permeabilized cardiac myocyte preparations (Kumar et al., 2015; Mamidi et al., 2016). Kumar et al. (2015) estimated the relative contribution of the PKA-mediated increase in length-dependent activation was 33% from cTnI phosphorylation and 67% from cMyBP-C phosphorylation. Taken together, these results implicate both cTnI and cMyBP-C in mediating the response of sarcomeric force to changes in length.

The current study tested whether cMyBP-C and its phosphorylation directly regulate PKA-mediated increases in power and the length dependence of power. Pseudo-phosphorylation at cMyBP-C PKA sites did not increase power per se above Control (Table 2) but did have a marked effect on length dependence of power (Fig. 2 and Fig. 3). In fact, length dependence of power was highly responsive to modified cMyBP-C; i.e., length dependence of power titrated with cMyBP-C pseudo-phosphorylation status. SL dependence of power progressively increased with the order of cMyBP-C KO = cMyBP-C t3SA < Control < cMyBP-C t3SD. We next tested whether this

continuum of length dependence of power translated to in vivo hearts by quantifying Frank-Starling relationships using a novel volume-loading technique in anesthetized mice. The progressive scale did not completely translate to in vivo hearts. However, consistent with length dependence of myofilament power, Frank-Starling relationships were significantly steeper in cMyBP-C t3SD mice. Overall, the results support the hypothesis that cMyBP-C and its phosphorylation tune SL dependence of myofibrillar power, and these regulatory processes translate across levels of myocardial organization to directly influence beat-to-beat ventricular performance.

Another interesting finding was that cMyBP-C pseudo-phosphorylation elicited greater changes in both myofibrillar length dependence of power and Frank-Starling relationships compared with Control than did cMyBP-C ablation compared with Control. This seems to be a paradoxical finding; however, myofilament mechanics clearly show that length dependence of power is diminished in the cMyBP-C KO myocytes. This likely arises from faster loaded shortening at short SLs especially at high loads (i.e., manifested as low curvature [higher a/Po values] of the force-velocity relationships), which translates to shallower Frank-Starling relationships. However, the in vivo slopes from cMyBP-C KO hearts were not statistically different than in Control. The reason(s) for this discrepancy between in vitro and in vivo results are uncertain but may involve (1) between-heart variability, (2) compensatory mechanisms such as alterations in end-diastolic volume dependence of myocyte length changes or intercell communication, and/or (3) group differences in end-diastolic volume (i.e., myocyte length) dependence of $[\text{Ca}^{2+}]_i$ handling. An important point from this study is that strain signal amplification (i.e., length dependence of myofilament power and steeper Frank-Starling relationships) involves cMyBP-C and its phosphorylation; i.e., cMyBP-C phosphorylation likely serves as a molecular amplifier of the length signal at multiple levels of myocardial organization.

Physiological and pathophysiological significance

Mammalian hearts exhibit a family of ventricular function curves, i.e., Frank-Starling relationships. For example, the Frank-Starling relationship shifts upward and becomes steeper in response to β -adrenergic stimulation (Sarnoff, 1955; Guyton et al., 1957). Conversely, the Frank-Starling relationship becomes depressed with heart failure (Jacob et al., 1992; Schwinger et al., 1994; Holubarsch et al., 1996), and interestingly, this coincides with down-regulation of the β -adrenergic signaling system (Bristow et al., 1982; Perrino and Rockman, 2007; Plegier et al., 2007). A plausible molecular regulator is cMyBP-C, since its phosphorylation state correlates with steepness of Frank-Starling relationships (Hanft et al., 2016). Consistent with this, several studies reported that the phosphorylation of cMyBP-C is reduced in failing rodent (Hanft et al., 2017) or human myocardium (Hamdani et al., 2008; Copeland et al., 2010; Kooij et al., 2010; Haynes et al., 2014; Stathopoulou et al., 2016). The present study showed that SL dependence of myofilament power is tightly regulated by cMyBP-C PKA phosphorylation sites, and these subcellular results translated to in vivo working hearts. These findings promise to motivate research that targets

cMyBP-C and its phosphorylation state as a potential therapeutic strategy in failing hearts, perhaps by developing small molecules that mimic cMyBP-C PKA phosphorylation (Bunch et al., 2019).

Acknowledgments

Henk L. Granzier served as editor.

This work was supported by National Institutes of Health grant HL57852 and a University of Missouri School of Medicine bridge grant to K.S. McDonald and National Institutes of Health grant HL139883 to R.L. Moss. The content is solely the responsibility of the authors and does not necessarily represent the official views of the National Institutes of Health.

The authors declare no competing financial interests.

Author contributions: L.M. Hanft and K.S. McDonald performed single cardiac myocyte preparation experiments. T.A. Hacker and D.P. Fitzsimons performed the in vivo cardiac ultrasound experiments. L.M. Hanft, D.P. Fitzsimons, T.A. Hacker, R.L. Moss, and K.S. McDonald contributed to data analysis and manuscript preparation.

Submitted: 25 September 2020

Revised: 4 January 2021

Accepted: 26 January 2021

References

Ait-Mou, Y., K. Hsu, G.P. Farman, M. Kumar, M.L. Greaser, T.C. Irving, and P.P. de Tombe. 2016. Titin strain contributes to the Frank-Starling law of the heart by structural rearrangements of both thin- and thick-filament proteins. *Proc. Natl. Acad. Sci. USA*. 113:2306–2311. <https://doi.org/10.1073/pnas.1516732113>

Allen, D.G., and S. Kurihara. 1982. The effects of muscle length on intracellular calcium transients in mammalian cardiac muscle. *J. Physiol.* 327: 79–94. <https://doi.org/10.1113/jphysiol.1982.sp014221>

Belknap, B., S.P. Harris, and H.D. White. 2014. Modulation of thin filament activation of myosin ATP hydrolysis by N-terminal domains of cardiac myosin binding protein-C. *Biochemistry*. 53:6717–6724. <https://doi.org/10.1021/bi500787f>

Braunwald, E., and J. Ross Jr. 1964. Applicability of Starling's law of the heart to man. *Circ. Res.* 15(Suppl 2):169–181.

Bristow, M.R., R. Ginsburg, W. Minobe, R.S. Cubicciotti, W.S. Sageman, K. Lurie, M.E. Billingham, D.C. Harrison, and E.B. Stinson. 1982. Decreased catecholamine sensitivity and beta-adrenergic-receptor density in failing human hearts. *N. Engl. J. Med.* 307:205–211. <https://doi.org/10.1056/NEJM198207223070401>

Bunch, T.A., R.S. Kanassatega, V.C. Lepak, and B.A. Colson. 2019. Human cardiac myosin-binding protein C restricts actin structural dynamics in a cooperative and phosphorylation-sensitive manner. *J. Biol. Chem.* 294: 16228–16240. <https://doi.org/10.1074/jbc.RA119.009543>

Cazorla, O., Y. Wu, T.C. Irving, and H. Granzier. 2001. Titin-based modulation of calcium sensitivity of active tension in mouse skinned cardiac myocytes. *Circ. Res.* 88:1028–1035. <https://doi.org/10.1161/hh1001.090876>

Chen, P.P., J.R. Patel, P.A. Powers, D.P. Fitzsimons, and R.L. Moss. 2012. Dissociation of structural and functional phenotypes in cardiac myosin-binding C conditional knockout mice. *Circulation*. 126:1194–1205. <https://doi.org/10.1161/CIRCULATIONAHA.111.089219>

Chung, J.H., B.L. Martin, B.D. Canan, M.T. Elnakish, N. Milani-Nejad, N.S. Saad, S.J. Repas, J.E.J. Schultz, J.D. Murray, J.L. Slabaugh, et al. 2018. Etiology-dependent impairment of relaxation kinetics in right ventricular end-stage failing human myocardium. *J. Mol. Cell. Cardiol.* 121: 81–93. <https://doi.org/10.1016/j.yjmcc.2018.07.005>

Colson, B.A., J.R. Patel, P.P. Chen, T. Bekyarova, M.I. Abdalla, C.W. Tong, D.P. Fitzsimons, T.C. Irving, and R.L. Moss. 2012. Myosin binding protein-C phosphorylation is the principal mediator of protein kinase A effects on

thick filament structure in myocardium. *J. Mol. Cell. Cardiol.* 53:609–616. <https://doi.org/10.1016/j.yjmcc.2012.07.012>

Copeland, O., S. Sadayappan, A.E. Messer, G.J. Steinen, J. van der Velden, and S.B. Marston. 2010. Analysis of cardiac myosin binding protein-C phosphorylation in human heart muscle. *J. Mol. Cell. Cardiol.* 49: 1003–1011. <https://doi.org/10.1016/j.yjmcc.2010.09.007>

de Tombe, P.P., R.D. Mateja, K. Tachampa, Y. Ait Mou, G.P. Farman, and T.C. Irving. 2010. Myofilament length dependent activation. *J. Mol. Cell. Cardiol.* 48:851–858. <https://doi.org/10.1016/j.yjmcc.2009.12.017>

Fuchs, F., and D.A. Martyn. 2005. Length-dependent Ca^{2+} activation in cardiac muscle: some remaining questions. *J. Muscle Res. Cell Motil.* 26: 199–212. <https://doi.org/10.1007/s10974-005-9011-z>

Fukuda, N., Y. Wu, G. Farman, T.C. Irving, and H. Granzier. 2003. Titin isoform variance and length dependence of activation in skinned bovine cardiac muscle. *J. Physiol.* 553:147–154. <https://doi.org/10.1113/jphysiol.2003.049759>

Grimm, A.F., H.-L. Lin, and B.R. Grimm. 1980. Left ventricular free wall and intraventricular pressure-sarcomere length distributions. *Am. J. Physiol.* 239:H101–H107. <https://doi.org/10.1152/ajpheart.1980.239.1.H101>

Guccione, J.M., W.G. O'Dell, A.D. McCulloch, and W.C. Hunter. 1997. Anterior and posterior left ventricular sarcomere lengths behave similarly during ejection. *Am. J. Physiol.* 272:H469–H477. <https://doi.org/10.1152/ajpheart.1997.272.1.H469>

Guyton, A.C., A.W. Lindsey, B. Abernathy, and J.B. Langston. 1957. Mechanism of the increased venous return and cardiac output caused by epinephrine. *Am. J. Physiol.* 192:126–130. <https://doi.org/10.1152/ajplegacy.1957.192.1.126>

Hamdani, N., M. de Waard, A.E. Messer, N.M. Boontje, V. Kooij, S. van Dijk, A. Versteilen, R. Lamberts, D. Merkus, C. Dos Remedios, et al. 2008. Myofilament dysfunction in cardiac disease from mice to men. *J. Muscle Res. Cell Motil.* 29:189–201. <https://doi.org/10.1007/s10974-008-9160-y>

Hanft, L.M., and K.S. McDonald. 2010. Length dependence of force generation exhibit similarities between rat cardiac myocytes and skeletal muscle fibres. *J. Physiol.* 588:2891–2903. <https://doi.org/10.1113/jphysiol.2010.190504>

Hanft, L.M., B.J. Biesiadecki, and K.S. McDonald. 2013. Length dependence of striated muscle force generation is controlled by phosphorylation of cTnI at serines 23/24. *J. Physiol.* 591:4535–4547. <https://doi.org/10.1113/jphysiol.2013.258400>

Hanft, L.M., T.D. Cornell, C.A. McDonald, M.J. Rovetto, C.A. Emter, and K.S. McDonald. 2016. Molecule specific effects of PKA-mediated phosphorylation on rat isolated heart and cardiac myofibrillar function. *Arch. Biochem. Biophys.* 601:22–31. <https://doi.org/10.1016/j.abb.2016.01.019>

Hanft, L.M., C.A. Emter, and K.S. McDonald. 2017. Cardiac myofibrillar contractile properties during the progression from hypertension to decompensated heart failure. *Am. J. Physiol. Heart Circ. Physiol.* 313: H103–H113. <https://doi.org/10.1152/ajpheart.00069.2017>

Harris, S.P., C.R. Bartley, T.A. Hacker, K.S. McDonald, P.S. Douglas, M.L. Greaser, P.A. Powers, and R.L. Moss. 2002. Hypertrophic cardiomyopathy in cardiac myosin binding protein-C knockout mice. *Circ. Res.* 90:594–601. <https://doi.org/10.1161/01.res.0000012222.70819.64>

Harris, S.P., B. Belknap, R.E. Van Sciver, H.D. White, and V.E. Galkin. 2016. C0 and C1 N-terminal Ig domains of myosin binding protein C exert different effects on thin filament activation. *Proc. Natl. Acad. Sci. USA*. 113:1558–1563. <https://doi.org/10.1073/pnas.1518891113>

Haynes, P., K.E. Nava, B.A. Lawson, C.S. Chung, M.I. Mitov, S.G. Campbell, A.J. Stromberg, S. Sadayappan, M.R. Bonnell, C.W. Hoopes, and K.S. Campbell. 2014. Transmural heterogeneity of cellular level power output is reduced in human heart failure. *J. Mol. Cell. Cardiol.* 72:1–8. <https://doi.org/10.1016/j.yjmcc.2014.02.008>

Hill, A.V. 1938. The heat of shortening and the dynamic constants of muscle. *Proc. R. Soc. Lond. B Biol. Sci.* 126:136–195. <https://doi.org/10.1098/rspb.1938.0050>

Hofmann, P.A., and F. Fuchs. 1987a. Effect of length and cross-bridge attachment on Ca^{2+} binding to cardiac troponin C. *Am. J. Physiol.* 253: C90–C96. <https://doi.org/10.1152/ajpcell.1987.253.1.C90>

Hofmann, P.A., and F. Fuchs. 1987b. Evidence for a force-dependent component of calcium binding to cardiac troponin C. *Am. J. Physiol.* 253: C541–C546. <https://doi.org/10.1152/ajpcell.1987.253.4.C541>

Holubarsch, C., T. Ruf, D.J. Goldstein, R.C. Ashton, W. Nickl, B. Pieske, K. Pioch, J. Lüdemann, S. Wiesner, G. Hasenfuss, et al. 1996. Existence of the Frank-Starling mechanism in the failing human heart. Investigations on the organ, tissue, and sarcomere levels. *Circulation*. 94: 683–689. <https://doi.org/10.1161/01.CIR.94.4.683>

- Jacob, R., B. Dierberger, and G. Kissling. 1992. Functional significance of the Frank-Starling mechanism under physiological and pathophysiological conditions. *Eur. Heart J.* 13(Suppl E):7–14. https://doi.org/10.1093/eurheartj/13.suppl_E.7
- Konhilas, J.P., T.C. Irving, and P.P. de Tombe. 2002. Myofilament calcium sensitivity in skinned rat cardiac trabeculae: role of interfilament spacing. *Circ. Res.* 90:59–65. <https://doi.org/10.1161/hh0102.102269>
- Konhilas, J.P., T.C. Irving, B.M. Wolska, E.E. Jweied, A.F. Martin, R.J. Solaro, and P.P. de Tombe. 2003. Troponin I in the murine myocardium: influence on length-dependent activation and interfilament spacing. *J. Physiol.* 547:951–961. <https://doi.org/10.1113/jphysiol.2002.038117>
- Kooij, V., M. Saes, K. Jaquet, R. Zaremba, D.B. Foster, A.M. Murphy, C. Dos Remedios, J. van der Velden, and G.J.M. Stienen. 2010. Effect of troponin I Ser23/24 phosphorylation on Ca^{2+} -sensitivity in human myocardium depends on the phosphorylation background. *J. Mol. Cell. Cardiol.* 48:954–963. <https://doi.org/10.1016/j.yjmcc.2010.01.002>
- Korte, F.S., K.S. McDonald, S.P. Harris, and R.L. Moss. 2003. Loaded shortening, power output, and rate of force redevelopment are increased with knockout of cardiac myosin binding protein-C. *Circ. Res.* 93:752–758. <https://doi.org/10.1161/01.RES.0000096363.85588.9A>
- Kumar, M., S. Govindan, M. Zhang, R.J. Khairallah, J.L. Martin, S. Sadayappan, and P.P. de Tombe. 2015. Cardiac myosin-binding protein C and troponin-I phosphorylation independently modulate myofilament length-dependent activation. *J. Biol. Chem.* 290:29241–29249. <https://doi.org/10.1074/jbc.M115.686790>
- Lee, K., S.P. Harris, S. Sadayappan, and R. Craig. 2015. Orientation of myosin binding protein C in the cardiac muscle sarcomere determined by domain-specific immuno-EM. *J. Mol. Biol.* 427:274–286. <https://doi.org/10.1016/j.jmb.2014.10.023>
- Luther, P.K., P.M. Bennett, C. Knupp, R. Craig, R. Padron, S.P. Harris, J. Patel, and R.L. Moss. 2008. Understanding the organisation and role of myosin binding protein C in normal striated muscle by comparison with MyBP-C knockout cardiac muscle. *J. Mol. Biol.* 384:60–72. <https://doi.org/10.1016/j.jmb.2008.09.013>
- Mamidi, R., K.S. Gresham, S. Verma, and J.E. Stelzer. 2016. Cardiac myosin binding protein-C phosphorylation modulates myofilament length-dependent activation. *Front. Physiol.* 7:38. <https://doi.org/10.3389/fphys.2016.00038>
- Mateja, R.D., and P.P. de Tombe. 2012. Myofilament length-dependent activation develops within 5 ms in guinea-pig myocardium. *Biophys. J.* 103:L13–L15. <https://doi.org/10.1016/j.bpj.2012.05.034>
- McDonald, K.S. 2000a. Ca^{2+} dependence of loaded shortening in rat skinned cardiac myocytes and skeletal muscle fibres. *J. Physiol.* 525:169–181. <https://doi.org/10.1111/j.1469-7793.2000.00169.x>
- McDonald, K.S. 2000b. Thin filament inactivation during isotonic shortening in skinned striated muscle preparations. *Biophys. J.* 78:225A.
- McDonald, K.S., and R.L. Moss. 1995. Osmotic compression of single cardiac myocytes eliminates the reduction in Ca^{2+} sensitivity of tension at short sarcomere length. *Circ. Res.* 77:199–205. <https://doi.org/10.1161/01.RES.77.1.199>
- Mun, J.Y., J. Gulick, J. Robbins, J. Woodhead, W. Lehman, and R. Craig. 2011. Electron microscopy and 3D reconstruction of F-actin decorated with cardiac myosin-binding protein C (cMyBP-C). *J. Mol. Biol.* 410:214–225. <https://doi.org/10.1016/j.jmb.2011.05.010>
- Mun, J.Y., M.J. Previs, H.Y. Yu, J. Gulick, L.S. Tobacman, S. Beck Previs, J. Robbins, D.M. Warshaw, and R. Craig. 2014. Myosin-binding protein C displaces tropomyosin to activate cardiac thin filaments and governs their speed by an independent mechanism. *Proc. Natl. Acad. Sci. USA.* 111:2170–2175. <https://doi.org/10.1073/pnas.1316001111>
- Mun, J.Y., R.W. Kensler, S.P. Harris, and R. Craig. 2016. The cMyBP-C HCM variant L348P enhances thin filament activation through an increased shift in tropomyosin position. *J. Mol. Cell. Cardiol.* 91:141–147. <https://doi.org/10.1016/j.yjmcc.2015.12.014>
- Perrino, C., and H.A. Rockman. 2007. Reversal of cardiac remodeling by modulation of adrenergic receptors: a new frontier in heart failure. *Curr. Opin. Cardiol.* 22:443–449. <https://doi.org/10.1097/HCO.0b013e3282294d72>
- Pleger, S.T., M. Boucher, P. Most, and W.J. Koch. 2007. Targeting myocardial beta-adrenergic receptor signaling and calcium cycling for heart failure gene therapy. *J. Card. Fail.* 13:401–414. <https://doi.org/10.1016/j.cardfail.2007.01.003>
- Pollack, G.H., and L.L. Huntsman. 1974. Sarcomere length-active force relations in living mammalian cardiac muscle. *Am. J. Physiol.* 227:383–389. <https://doi.org/10.1152/ajplegacy.1974.227.2.383>
- Ponnam, S., I. Sevrieva, Y.B. Sun, M. Irving, and T. Kampourakis. 2019. Site-specific phosphorylation of myosin binding protein-C coordinates thin and thick filament activation in cardiac muscle. *Proc. Natl. Acad. Sci. USA.* 116:15485–15494. <https://doi.org/10.1073/pnas.1903033116>
- Rosas, P.C., Y. Liu, M.I. Abdalla, C.M. Thomas, D.T. Kidwell, G.F. Dusio, D. Mukhopadhyay, R. Kumar, K.M. Baker, B.M. Mitchell, et al. 2015. Phosphorylation of cardiac Myosin-binding protein-C is a critical mediator of diastolic function. *Circ. Heart Fail.* 8:582–594. <https://doi.org/10.1161/CIRCHEARTFAILURE.114.001550>
- Sarnoff, S.J. 1955. Myocardial contractility as described by ventricular function curves; observations on Starling's law of the heart. *Physiol. Rev.* 35:107–122. <https://doi.org/10.1152/physrev.1955.35.1.107>
- Schwinger, R.H., M. Böhm, A. Koch, U. Schmidt, I. Morano, H.J. Eissner, P. Überfuhr, B. Reichart, and E. Erdmann. 1994. The failing human heart is unable to use the Frank-Starling mechanism. *Circ. Res.* 74:959–969. <https://doi.org/10.1161/01.RES.74.5.959>
- Stathopoulou, K., I. Wittig, J. Heidler, A. Piasecki, F. Richter, S. Diering, J. van der Velden, F. Buck, S. Donzelli, E. Schröder, et al. 2016. S-glutathiolation impairs phosphoregulation and function of cardiac myosin-binding protein C in human heart failure. *FASEB J.* 30:1849–1864. <https://doi.org/10.1096/fj.201500048>
- Stelzer, J.E., S.B. Dunning, and R.L. Moss. 2006. Ablation of cardiac myosin-binding protein-C accelerates stretch activation in murine skinned myocardium. *Circ. Res.* 98:1212–1218. <https://doi.org/10.1161/01.RES.0000219863.94390.ce>
- Stelzer, J.E., J.R. Patel, J.W. Walker, and R.L. Moss. 2007. Differential roles of cardiac myosin-binding protein C and cardiac troponin I in the myofibrillar force responses to protein kinase A phosphorylation. *Circ. Res.* 101:503–511. <https://doi.org/10.1161/CIRCRESAHA.107.153650>
- Tachampa, K., H. Wang, G.P. Farman, and P.P. de Tombe. 2007. Cardiac troponin I threonine 144: role in myofilament length dependent activation. *Circ. Res.* 101:1081–1083. <https://doi.org/10.1161/CIRCRESAHA.107.165258>
- Tong, C.W., J.E. Stelzer, M.L. Greaser, P.A. Powers, and R.L. Moss. 2008. Acceleration of crossbridge kinetics by protein kinase A phosphorylation of cardiac myosin binding protein C modulates cardiac function. *Circ. Res.* 103:974–982. <https://doi.org/10.1161/CIRCRESAHA.108.177683>
- Tong, C.W., X. Wu, Y. Liu, P.C. Rosas, S. Sadayappan, A. Hudmon, M. Muthuchamy, P.A. Powers, H.H. Valdivia, and R.L. Moss. 2015. Phosphoregulation of cardiac inotropy via myosin binding protein-C during increased pacing frequency or β 1-adrenergic stimulation. *Circ. Heart Fail.* 8:595–604. <https://doi.org/10.1161/CIRCHEARTFAILURE.114.001585>
- Wang, Y.P., and F. Fuchs. 1995. Osmotic compression of skinned cardiac and skeletal muscle bundles: effects on force generation, Ca^{2+} sensitivity and Ca^{2+} binding. *J. Mol. Cell. Cardiol.* 27:1235–1244. [https://doi.org/10.1016/S0022-2828\(05\)82385-5](https://doi.org/10.1016/S0022-2828(05)82385-5)